Potential energy curves of M($np\ ^2P$)·RG($^2\Pi$) excited states and M$^+$·RG ground states (M=Li, Na; RG=He, Ne)

Solomon Bililign,[a] Maciej Gutowski,[b] Jack Simons, and W. H. Breckenridge
Department of Chemistry, University of Utah, Salt Lake City, Utah 84112

(Received 17 September 1993; accepted 24 February 1994)

It has been established for some time that the bond energies for any given valence $p\pi$ excited state of Group 1 (^2P) and Group 2 ($^{1,3}P$) metal-atom/rare-gas (M·RG) van der Waals complexes tend to increase with the polarizability of the RG atom. It is also known that the binding energies of the corresponding M$^+$·RG ground state ions are generally *greater* than those of the neutral M($p\pi$)·RG excited states with the same RG atom. However, there are *two stark exceptions* to these trends, both involving Group 1 metal atoms and the rare gas He; Li($2p\ ^2P$)·He($^2\Pi$) and Na($3p\ ^2P$)·He($^2\Pi$), which are the focus of the present study. We have conducted *ab initio* calculations of the potential energy curves of M($np\ ^2P$)·RG($^2\Pi$) and M$^+$·RG states, where M=Li, Na and RG=He, Ne. We find that the unusual behavior of the $p\pi$ Group 1 metal atom states is due to (i) the lack of M($p\pi$)–RG($p\pi$) repulsive orbital overlap in the He case, and (ii) substantial *additional* attraction due to correlated motion of the RG atom's electrons and the diffuse M($np\pi$) electron which is absent in the M$^+$RG cases.

I. INTRODUCTION

Many excited electronic states of metal-atom/rare-gas (M·RG) van der Waals complexes have now been characterized experimentally. An interesting class of such complexes are those of Group 1, 2, and 12 metal atoms in which a ground-state *ns* electron has been excited (experimentally, usually by laser excitation) to a *valence np* orbital.[1–49] The binding character of the M(np)·RG or M($nsnp$)·RG excited states depends dramatically on the alignment of the *np* orbital with respect to the internuclear axis. Sigma alignment of the *np* orbital is more favorable at very long range, where the axial $np\sigma$ electron density provides a greater dispersive attraction. However, M($np\sigma$)·RG(σ) electron–electron repulsion *also* sets in at very large distances; therefore the M($np\sigma$)·RG and M($nsnp\sigma$)·RG states are *essentially repulsive* but have very shallow potential minima at large R_e values. In contrast, for pi alignment of the M(np) orbital, because the RG atom is approaching along the $np\pi$ orbital nodal axis, electron–electron repulsion does not become appreciable until much smaller values of R. The RG atom can thus penetrate much closer to the M$^+$ core and experience strong ion–induced-dipole-like attractive forces. Therefore, the M($np\pi$)·RG and M($nsnp\pi$)·RG states are more strongly bound.

Shown in Table I are R_e and D_e data for a series of such complexes.[1–49] Included for comparisons are similar values for analogous ground-state M$^+$·RG complexes for which R_e and D_e have either been estimated experimentally or calculated by *ab initio* techniques. There are *two clear trends* in D_e values which can be discerned from the π state and M$^+$·RG data in Table I.

First, for a given metal atom state, the D_e values tend to increase in the order He, Ne, Ar, Kr, Xe. This is expected, of course, since the polarizability of the RG atom increases in this order, and any attractive interaction [M($p\pi$)·RG dispersion, M$^+$(core)·RG ion/induced-dipole, etc.] will increase with RG polarizability. Analogous trends are also observed in M·RG ground state D_e values, and in excited M(Rydberg)·RG D_e values.[50] However, there are two glaring *exceptions*, both for Group 1 metal atoms with RG=He: Li($2p\ ^2P_{3/2}$)·He($^2\Pi_{3/2}$), and Na($3p\ ^2P_{3/2}$)·He($^2\Pi_{3/2}$) (see Table I).

The second clear trend is that the D_e values for M$^+$·RG ions are greater than for the analogous valence $p\pi$ excited M·RG states. This trend makes sense, since in the neutral Π states, the $np\pi$ electron is partially shielding the M$^+$ "core." However, there are two *exceptions* to this trend, again involving Li($2p\ ^2P_{3/2}$)·He($^2\Pi_{3/2}$), and Na($3p\ ^2P_{3/2}$)·He($^2\Pi_{3/2}$)! (See Table I and the discussion below.)

The unexpectedly high binding energies of the valence $np\pi$ states of Li·He and Na·He is quite interesting and was the basis of the work reported here. As detailed below, we find that the exceptional behavior apparently has to do *both* with He being the RG atom *as well* as the Group 1 nature of Li and Na, since the $np\pi$ excited states of Mg·He (Group 2) and Hg·He (Group 12) complexes, for example, are less bound than the analogous complexes for RG=Ne. (See Table I.) We also note particularly the *astounding* difference in the D_e values for the $p\pi$ state of Na·He($^2\Pi$) (~490 cm^{-1}) compared to the analogous $p\pi$ state of Mg·He($^3\Pi$) (~15 cm^{-1})!

The binding differences between the excited $p\pi$ M·He states of Group 1 versus Group 2, 12 metal atoms is easy to rationalize *qualitatively*.[50] The M$^+$ cores of Group 1 $np\pi$ states are very small compared to their group 2 or group 12 analogs, which have an *ns valence* orbital occupied. For example, the mean radius of a $3s$ electron in the Mg atom is 1.72 Å, compared to the mean radius of a Na$^+$ ion of only 0.42 Å.[51] This means that a He atom can penetrate much closer to the M$^+$ core for, say, the Na($3p\pi$) state than for the

---

[a] Present address: Department of Physics, North Carolina A&T State University, Greensboro, NC 27411.

[b] Present address: IBM Research Division, Almaden Research Center, 650 Harry Road, San Jose, CA 95120-6099.

0021-9606/94/100(11)/8212/7/$6.00

TABLE I. M·RG valence excited states and M^+·RG ground states. (M=Group 1, 2, 12 metal atoms; RG=rare gas atoms.) D_e values in cm^{-1}; R_e values in Å.

Metal atom atomic state	Molecular state	M·He		M·Ne		M·Ar		M·Kr		M·Xe	
		D_e	R_e	D_e	R_e	D_e	R_e	D_e	R_e	D_e	R_e
$\mathrm{Li}(2p\ ^2P_{3/2})$	$^2\Pi_{3/2}$	1020^{a}	1.78^{a}	212^{b}	2.31^{b}	[800]^{c}	[3.1]^{c}	[1180]^{c}	[3.2]^{c}	[1630]^{c}	[3.1]^{c}
		(868)^{d}	(1.81)^{d}								
$\mathrm{Li}^+(1s^2\ ^1S_0)$	$^1\Sigma^+$	[596]^{e}	[1.96]^{e}	[920]^{f}	[2.11]^{f}	[2173]^{g}	[2.40]^{g}	[3183]^{g}	[2.42]^{g}	[4310]^{f}	[2.54]^{f}
		[570]^{f}	[1.96]^{f}	[968]^{h}	[2.06]^{h}	[2195]^{k}	[2.43]^{k}	[3710]^{f}	[2.45]^{f}	[4434]^{g}	[2.51]^{g}
		[593]^{g}	[1.93]^{g}	[1034]^{i}	[1.99]^{i}	[2520]^{f}	[2.42]^{f}	(2490)^{n}	(2.56)^{n}		
		(601)^{d}	(1.92)^{d}	(1001)^{j}	(2.04)^{j}	(2040)^{l}	(2.42)^{l}				
						(2190)^{m}	(2.38)^{m}				
$\mathrm{Be}^+(1s^22s\ ^2S_{1/2})$	$^2\Sigma^+_{1/2}$					4100^{o}	2.09^{o}	[5400]^{p}	2.22^{p}		
$\mathrm{Na}(3p\ ^2P_{3/2})$	$^2\Sigma^+$			4.5^{q,r}	7.9^{q,r}						
$\mathrm{Na}(3p\ ^2P_{3/2})$	$^2\Pi_{3/2}$	[480]^{s}	[2.3]^{s}	144^{q,r}	2.73^{q,r}	568$^{\Delta,u}$	2.91$^{\Delta,u}$	760^{v}	3.05^{v}	1120^{w}	3.22^{w}
		(496)^{t}	(2.30)^{t}								
$\mathrm{Na}^+(2p^6\ ^1S_0)$	$^1\Sigma^+$	[285]^{f}	[2.41]^{f}	[520]^{f}	[2.49]^{f}	[1504]^{f}	[2.70]^{f}	[1778]^{y}	[2.91]^{y}	[2079]^{y}	[2.98]^{y}
		(266)^{x}	(2.41)^{x}	(508)^{x}	(2.48)^{x}	(1150)^{x}	(2.86)^{x}	[1774]^{f}	[2.87]^{f}	[2089]^{f}	[3.11]^{f}
						(1020)^{l}	(2.88)^{l}				
						(1310)^{i}	(2.77)^{i}				
$\mathrm{Mg}(3s3p\ ^3P_1)$	$^3\Pi_{0^+}$	(15)^{z}	(4.2)^{z}			316^{†,bb}	3.63^{bb}				
		(16)^{aa}	(4.2)^{aa}								
$\mathrm{Mg}(3s3p\ ^1P_1)$	$^1\Pi_1$			53^{cc}	3.85^{cc}	368^{dd}	3.27^{dd}			1500^{ee}	3.07^{ee}
$\mathrm{Mg}^+(3s\ ^2S_{1/2})$	$^2\Sigma^+_{1/2}$	(73)^{x}	(3.57)^{x}	(169)^{x}	(3.30)^{x}	1270^{ff}					
						1187^{ff}					
						(1073)^{l}	(2.88)^{l}				
						(1137)^{x}	(2.89)^{x}				
$\mathrm{Zn}(4s4p\ ^3P_2)$	$^3\Pi_2$					487^{†,gg}	3.23^{gg}				
$\mathrm{Zn}(4s4p\ ^1P_1)$	$^1\Sigma^+$									134±12^{hh}	[5.9]^{hh}
$\mathrm{Zn}(4s4p\ ^1P_1)$	$^1\Pi_1$					706^{ii}	2.97^{ii}	1466^{jj}	2.79^{jj}	3241^{hh}	[2.8]^{hh}
$\mathrm{Cd}(5s5p\ ^3P_1)$	$^3\Pi_{0^+}$			77^{kk}	3.62^{kk}	322^{ll},325^{kk}	3.45^{kk}	513^{kk}		1086^{kk}	
								[499]^{mm}			
$\mathrm{Cd}(5s5p\ ^3P_2)$	$^3\Pi_2$					435^{†,nn}	3.37^{nn}				
$\mathrm{Cd}(5s5p\ ^1P_1)$	$^1\Pi_1$			89^{oo}	3.61^{oo}	544^{oo}	3.28^{oo}	1036^{oo}			
$\mathrm{Hg}(6s6p\ ^3P_1)$	$^3\Pi_{0^+}$	22^{pp}	3.46^{pp}	83^{pp}	3.47^{pp}	376^{pp}	3.36^{pp}	629^{qq}	[3.35]^{qq}	1381^{qq}	[3.15]^{qq}
$\mathrm{Hg}(6s6p\ ^3P_2)$	$^3\Pi_2$					437^{pp}	3.31^{rr}				
$\mathrm{Hg}(6s6p\ ^1P_1)$	$^1\Pi_1$			96^{ss}	3.41^{ss}	542^{ss}	3.28^{ss}	1495^{ss}	[2.93]^{ss}	[3595]^{ss}	[2.95]^{ss}
$\mathrm{Hg}^+(6s\ ^2S_{1/2})$	$^2\Sigma^+$					1840±37^{tt}		3170^{ww}		6033^{ww}	
						[1630±100]^{uu}	[<2.87]^{uu}				
						>1800^{vv}					

[†] Probably upper limits: Possible maxima in $^3\Sigma^+$ or $^2\Sigma^+$ "Rydberg-state" potentials of upper states in spectroscopic transitions. $^{\Delta 2}\Pi_{1/2}$.

( ):From a theoretical calculation of potential curve.

[ ]:Estimated value, a value which has been determined indirectly, or a value which is relatively uncertain, we believe.

[a] Reference 1.
[b] Reference 2.
[c] Reference 3.
[d] Reference 4.
[e] Reference 5.
[f] Reference 6.
[g] Reference 7.
[h] Reference 8.
[i] Reference 9.
[j] Reference 10.
[k] Reference 11.
[l] Reference 12.
[m] Reference 13.
[n] Reference 14.
[o] Reference 15.
[p] Reference 16.
[q] Reference 17.
[r] Reference 18.
[s] Reference 19.
[t] Reference 20.
[u] Reference 21.
[v] Reference 22.
[w] Reference 23.
[x] Reference 24.
[y] Reference 25.
[z] Reference 26.
[aa] Reference 27.
[bb] Reference 28.
[cc] Reference 29.
[dd] Reference 30.
[ee] Reference 31.
[ff] Reference 32.
[gg] Reference 33.
[hh] Reference 34.
[ii] Reference 35.
[jj] Reference 36.
[kk] Reference 37.
[ll] Reference 38.
[mm] Reference 39.
[nn] Reference 40.
[oo] Reference 41.
[pp] Reference 42.
[qq] Reference 43.
[rr] Reference 44.
[ss] Reference 45.
[tt] Reference 46.
[uu] Reference 47.
[vv] Reference 48.
[ww] Reference 49.

$\mathrm{Mg}(3s3p\pi)$ state. The D_e values for Na^+·He, ~280 cm^{-1} at $R_e \approx 2.4$ Å, versus Mg^+·He, ~70 cm^{-1} at $R_e \approx 3.6$ Å (see Table I), are consistent with this idea.

One aspect of the D_e and R_e trends that is *difficult to explain* is why, when interacting with *np* M atom states, the Ne atom yields so much larger R_e values than the He atom even though the Ne atom is not that much larger than the He atom. For example, the mean radius of the $1s$ electrons in He is 0.49 Å, while that of the $2p$ electrons in Ne is only 0.51 Å.[51] Also, estimates of the "hard-sphere" radius of the helium atom are ~1.3 Å vs ~1.4 Å for the neon atom.[52] Finally, as shown in Table I, when the np orbital is empty, the estimated R_e values for the $Li^+ \cdot He$ and $Na^+ \cdot He$ ions are not much smaller than the R_e values for the $Li^+ \cdot Ne$ and $Na^+ \cdot Ne$ ions, respectively. Another aspect that is not easy to rationalize is why $Na(3p\ ^2P) \cdot He(^2\Pi)$ and $Li(2p\ ^2P) \cdot He(^2\Pi)$ are even more *strongly* bound, and have shorter R_e values, than $Na^+ \cdot He$ and $Li^+ \cdot He$, as seen in Table I.

The resolution of both of the above questions suggested by the data obtained in this study is that (i) repulsion between the diffuse $M(np\pi)$ electron and the RG atom is very small for He but not so for Ne, and (ii) there exist attractive dispersive interactions between the $M(np\pi)$ electron and the He or Ne atom's electrons that are absent in the M^+RG cases. The balance that is established between attractive and repulsive interactions leads to a shorter R_e and larger D_e for $MHe(^2\Pi)$ than for $MNe(^2\Pi)$, primarily because of the significantly weaker repulsion in $MHe(^2\Pi)$. This balance leads to smaller R_e and larger D_e values for $MHe(^2\Pi)$ than for M^+He because of the dispersive attraction present in the $MHe(^2\Pi)$ cases.

TABLE II. Constitution of the MCSCF/MRCI wave function.

	MCSCF space	
Species	FC[a]	Active[b]
LiHe	$1s_{Li}$	$1s_{He}, 2s_{Li}, 2p_{Li}$
LiNe	$1s_{Li}, 1s_{Ne}$	$2s_{Ne}, 2p_{Ne}, 2s_{Li}, 2p_{Li}$
NaNe	$1s_{Ne}, 1s_{Na}, 2s_{Na}, 2p_{Na}$	$2s_{Ne}, 2p_{Ne}, 3s_{Na}, 3p_{Na}$
NaHe	$1s_{Na}, 2s_{Na}, 2p_{Na}$	$1s_{He}, 3s_{Na}, 3p_{Na}$

[a] Frozen core orbitals, i.e., orbitals which are doubly occupied in every configuration state function.

[b] Orbitals among which the valence electrons are distributed in all possible ways to form a *reference space* for the CI (single and double excitation) calculation.

We report here *ab initio* calculations of the potential curves of the $Li(2p\ ^2P) \cdot He(^2\Pi)$ and $Na(3p\ ^2P) \cdot He(^2\Pi)$ states, and for comparison, the potential curves of the $Li^+(1s^2\ ^1S_0) \cdot He(^1\Sigma^+)$ and $Na^+(2p^6\ ^1S_0) \cdot He(^1\Sigma^+)$ ionic states. Calculations with the Ne atom replacing the He atom were also carried out (or have been performed by others[10]). The results of these calculations, our analysis of them, and a discussion of van der Waals bonding in such M·RG and $M^+ \cdot RG$ states, are presented.

II. THEORETICAL METHODOLOGY

The electronic ground states of closed-shell $Li^+ \cdot He$, $Na^+ \cdot He$, and $Na^+ \cdot Ne$ ions were described by the quadratic configuration interaction including single and double excitations with approximate treatment of triple excitations based on a self-consistent field (SCF) reference function [QCISD(T)], implemented via the GAUSSIAN 92 code.[53] All valence electrons were correlated. For Li^+Ne, a high quality potential curve was available,[10] so we merely verified its accuracy.

The first $^2\Pi$ excited states ($^2B_1$ in C_{2v} symmetry) of Li·He, Li·Ne, Na·He, and Na·Ne were described by complete active space (CAS) self-consistent field (SCF) multireference configuration interaction (MRCI) wave functions, implemented via the GAMESS code.[54] The constitution of the configuration spaces used is given in Table II. The basis sets used for each calculation are listed in Table III.[55–64] The QCI and MCSCF/MRCI interaction energies were corrected for the basis set superposition error using the function counterpoise procedure,[65] and the MCSCF/MRCI interaction energies were corrected for size-inconsistency error by using the supermolecule to compute the asymptotic energies.[66]

All of the *ab initio* calculations were performed on our IBM RISC System 6000 350 workstations.

TABLE III. Basis sets used in the *ab initio* calculations.

System	State	Basis set
Li^+He	$^1\Sigma^+$	6–311G[a] plus three p (He) and three d (Li); splitting factors (4,1,0.25),[b] exponents 0.75 (p), 0.2 (d)
LiHe	$^2\Pi$	
Li^+Ne	$^1\Sigma^+$	DZV[c] with one p (0.076) on Li and one d (1.883) on Ne[d]
Na^+He	$^1\Sigma^+$	6–311 G**[a,e]
Na^+Ne	$^1\Sigma^+$	Ne: as in Li^+Ne; Na: HW[f] plus one p (0.061)
LiNe	$^2\Pi$	SBK[g] plus two d on Ne (0.852, 4550)[d] plus four diffuse d's on Li, exponents 0.9, 0.2723, 0.0842, 0.0210[j]
NaHe	$^2\Pi$	He: as in LiHe; Na: 6–311 G plus three d, exponent 0.175, splitting factors (4,1,0.25)[b]
NaNe	$^2\Pi$	TZV[e,h] plus three d; splitting factors (4,1,0.25), exponents 2.0 (Ne) and 0.157 (Na)[i]
LiNe	$^2\Delta$	As in LiNe ($^2\Pi$)

[a] Reference 55.
[b] Reference 62.
[c] Reference 57.
[d] Reference 59.
[e] Reference 56.
[f] Reference 58.
[g] Reference 63.
[h] Reference 60.
[i] Reference 61.
[j] Reference 64.

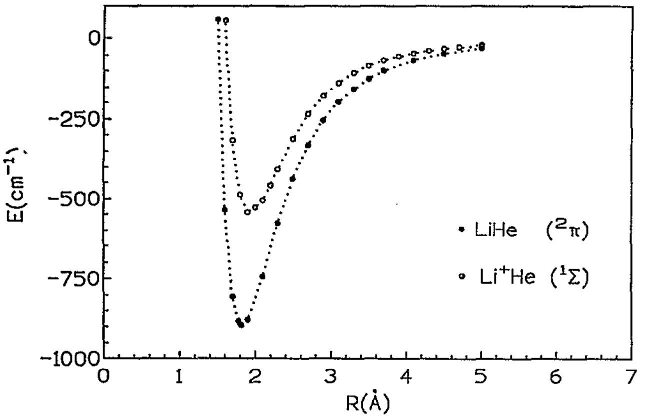

FIG. 1. Calculated potential curves of the excited Li·He($^2\Pi$) and the Li$^+$·He($^1\Sigma^+$) ground state. See the text.

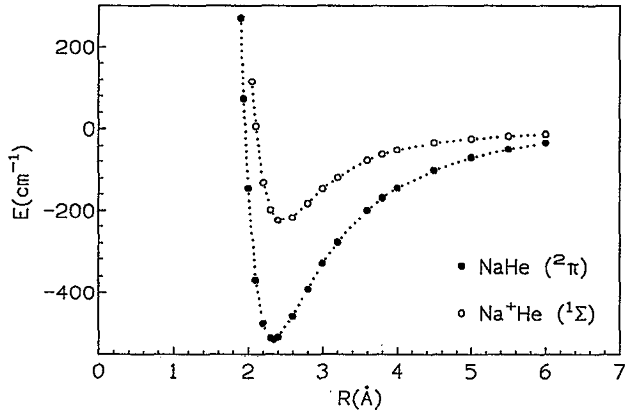

FIG. 3. Calculated potential curves of the excited Na·He($^2\Pi$) and the Na$^+$·He($^1\Sigma^+$) ground state. See the text.

III. RESULTS AND DISCUSSION

A. Comparing $^2\Pi$ states of M·RG to the ground states of M$^+$RG

Shown in Figs. 1–4 are potential curves calculated for the $^2\Pi$ excited states of the van der Waals molecules of interest and the corresponding ground-state cations. The fact that neutral LiHe and NaHe are *more* strongly bound than their corresponding cations while LiNe and NaNe are *less* strongly bound than their cations is strikingly illustrated in these figures.

Shown in Table IV are D_e and R_e values extracted from our calculations, along with similar values from earlier experimental and theoretical studies for comparison purposes. It can be seen that our calculated R_e and D_e values are reasonably consistent with both the experimental estimates and with the findings of other *ab initio* calculations. In fact, our calculated results in some cases may be only in fortuitously good agreement with the experimental data given the modest basis sets and configuration spaces employed, but the main purpose of our calculations is to obtain a qualitative understanding of the bonding in these states.

The fact that the R_e values for Li$^+$He vs Li$^+$Ne (and Na$^+$He vs Na$^+$Ne) agree within ~0.1 Å (see Table IV), as do the He and Ne hard-sphere radii,[52] indicates that the intrinsic "size" of Ne is not much larger than that of He, as stated earlier. When interacting with the *closed-shell* cations (Li$^+$ and Na$^+$), the He and Ne atoms behave as though their sizes are quite similar, so the intrinsic sizes of the rare gas atoms are not what causes M·He($^2\Pi$) to be more strongly bound than MNe($^2\Pi$).

B. Origin of the strong binding in the Li·He($^2\Pi$) and Na·He($^2\Pi$) states

It was long ago recognized by Krauss *et al.*[68] that the anomalously strong SCF binding in MHe($^2\Pi$) might be caused by the lack of overlap between the diffuse $p\pi$ orbital of M and the occupied $1s$ orbital of He. In contrast, when Ne replaces He, there exists strong overlap between the M($np\pi$) orbital and Ne's $p\pi$ orbitals. The resultant lack of M($p\pi$)–RG($p\pi$) repulsion for He allows a much closer ap-

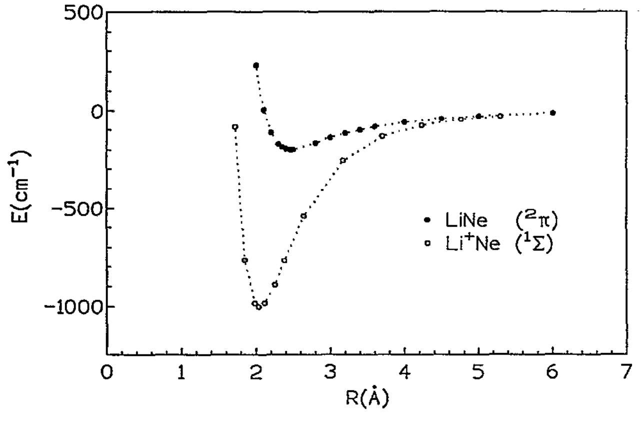

FIG. 2. Calculated potential curves of the excited Li·Ne($^2\Pi$) and the Li$^+$·Ne($^1\Sigma^+$) ground state. The Li$^+$·Ne($^1\Sigma^+$) points are from Ref. 10. See the text.

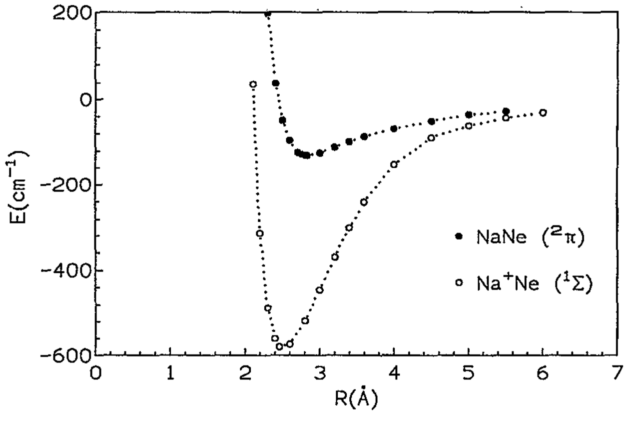

FIG. 4. Calculated potential curves of the excited Na·Ne($^2\Pi$) and the Na$^+$·Ne($^1\Sigma^+$) ground state. See the text.

TABLE IV. Dissociation energies and equilibrium internuclear distances of the states of interest.

	D_e (cm^{-1})		R_e (Å)	
State	Theory	Expt.[a]	Theory	Expt.[a]
$\mathrm{Li\cdot He}(^2\Pi)$	894^b	1020	1.82^b	1.78
	868^c		1.81^c	
$\mathrm{Li\cdot Ne}(^2\Pi)$	200^b	212	2.47^b	2.31
	214^g		2.26^g	
$\mathrm{Li^+\cdot He}(^1\Sigma^+)$	546^b	[~580]	1.95^b	[~1.95]
	601^c		1.92^c	
$\mathrm{Li^+\cdot Ne}(^1\Sigma^+)$	1001^d	[~950]	2.04^d	[~2.05]
$\mathrm{Na\cdot He}(^2\Pi)$	513^b	[~480]	2.34^b	[~2.3]
	496^e		2.30^e	
$\mathrm{Na\cdot Ne}(^2\Pi)$	131^b	144	2.83^b	2.73
$\mathrm{Na^+\cdot He}(^1\Sigma^+)$	225^b	[~285]	2.41^b	[~2.4]
	266^f		2.41^f	
$\mathrm{Na^+\cdot Ne}(^1\Sigma^+)$	580^b	[~520]	2.48^b	[~2.5]
	508^f		2.48^f	

[a] Taken from Table I. Values in brackets are from one or more estimates which probably have greater uncertainty than the spectroscopically determined values.
[b] This work.
[c] Reference 4.
[d] Reference 10.
[e] Reference 20.
[f] Reference 24.
[g] Reference 67.

proach to the He atom than to the Ne atom, thereby allowing the M($p\pi$) species to experience an interaction much like that in the M^+–He ions (in fact, even *stronger*, as discussed in the following paragraph).

Although the overlap argument may rationalize the differences between $\mathrm{M\cdot Ne}(^2\Pi)$ and $\mathrm{M\cdot He}(^2\Pi)$, it does not explain why the $\mathrm{Li\cdot He}(^2\Pi)$ and $\mathrm{Na\cdot He}(^2\Pi)$ excited states are substantially *more* bound than the cationic $\mathrm{Li^+\cdot He}$ and $\mathrm{Na^+\cdot He}$ ground states, respectively. Our data (specifically, the difference between the SCF and the correlated-level potentials; see Table V) indicate an additional attraction, due to the $p\pi$ orbital of M interacting with the RG atom. At the shorter R_e of $\mathrm{MHe}(^2\Pi)$, this dispersive attractive interaction is quite substantial; for Ne, with its larger R_e, the same attractive interaction is present but its magnitude is smaller.

TABLE V. Comparison of R_e (Å), D_e (cm^{-1}) values for SCF calculations versus calculations with correlation.

	SCF		Calculations with correlation	
	R_e	D_e	R_e	D_e
$\mathrm{Li}(2p\ ^2P)\cdot\mathrm{He}(^2\Pi)$	1.95^a	506^a	1.82^a	894^a
	1.88^b	525^b	1.81^b	868^b
	$\sim1.9^c$	$\sim520^c$		
$\mathrm{Li^+\cdot He}(^1\Sigma^+)$	1.98^a	510^a	1.95^a	546^a
	1.94^b	554^b	1.92^b	601^b
	$\sim2.0^c$	$\sim520^c$		
$\mathrm{Li}(2p\ ^2P)\cdot\mathrm{Ne}(^2\Pi)$	(Unbound)[a]		2.47^a	200^a
			2.26^e	212^e
$\mathrm{Li^+\cdot Ne}(^1\Sigma^+)$	2.04^d	859^d	2.04^d	1001^d

[a] This work.
[b] Reference 4.
[c] Reference 69.
[d] Reference 10.
[e] Reference 67.

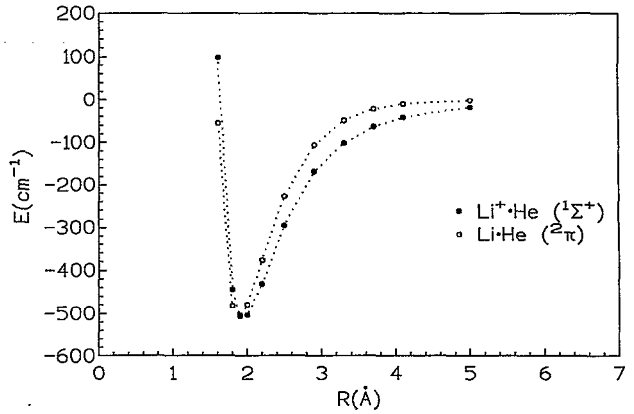

FIG. 5. SCF energies calculated for the excited $\mathrm{Li}(2p\ ^2P)\cdot\mathrm{He}(^2\Pi)$ and the $\mathrm{Li^+\cdot He}(^1\Sigma^+)$ ground state and the $\mathrm{Li^+\cdot He}(^1\Sigma^+)$ ion. See the text.

To illustrate, the self-consistent field (SCF) interaction potentials for $\mathrm{Li^+He}$ and $\mathrm{LiHe}(^2\Pi)$ are compared in Fig. 5, where they are seen to be much more alike[68] than are the corresponding correlated potentials shown in Fig. 1, consistent with there being an additional attraction present in $\mathrm{LiHe}(^2\Pi)$ compared to $\mathrm{Li^+He}$. Although the correlation interaction energy involved (~380 cm^{-1}) might seem at first too large for dispersion-type interactions for an atom like He with such a small polarizability, the Li($2p\pi$) orbital has a very large polarizability and the internuclear interaction distances (~1.8 Å) are *much* smaller than usually encountered for net attractive dispersion-type interactions.

The C_6 coefficient for the $p\pi$ interaction of $\mathrm{Li}(2p\ ^2P_J)$ with the He atom has been calculated[70] to be 0.273×10^{-58} erg cm^6. For $R=1.82$ Å, this would lead to an attractive energy of -3800 cm^{-1}, more than sufficient to account for the correlation energy of -390 cm^{-1}. The profound discrepancy between the C_6/R^6 multipole-approximated dispersive interaction and the *ab initio* evaluated correlation energy term has its origin in the "dampening" arising from the interpenetration of the instantaneous multipole densities [i.e., penetration of the Li($p\pi$) and He $1s$ orbitals].[71] Due to the unusually short M–He distances, the dampening is expected to be large. A crude estimate of the interpenetration effects can be obtained if we consider the effective center of charge of the "lobes" resulting from the transverse Li($2p\pi$) orbital. A Li($2p\pi$)·He distance of only ~2.7 Å would be required to produce a dispersive attraction of 390 cm^{-1}, and this would correspond to an effective dispersion "center of charge" of the Li($2p\pi$) orbital (as measured from the Li nucleus in a direction perpendicular to the Li·He bond axis) of ~2.0 Å, which is certainly of the right order.

C. More details on the origin of the M$p\pi$–Ne repulsion

The qualitative difference between the $^2\Pi$ complexes of He vs Ne manifests itself even at the SCF level, as shown in Table V and Figs. 5 and 6 (analogous data is obtained when Na replaces Li). The SCF interaction energy, $E_{\mathrm{int}}^{\mathrm{SCF}}$, is attrac-

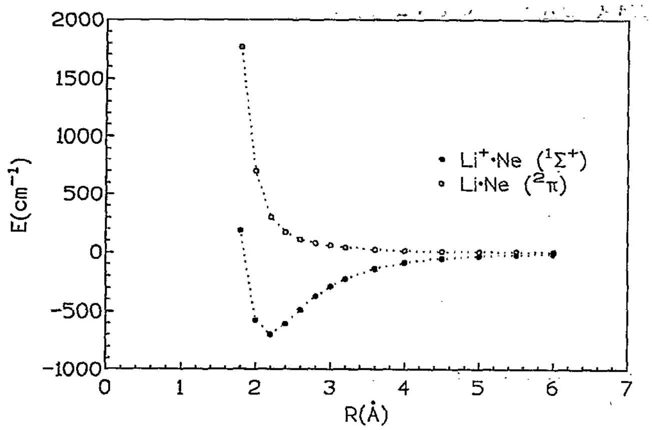

FIG. 6. Same as Fig. 5, but for the Li($2p$ ^2P)·Ne($^2\Pi$) state and the Li$^+$·Ne($^1\Sigma^+$) ion.

tive over a wide range of R for MHe($^2\Pi$) and is similar to the M$^+$He $E_{\rm int}^{\rm SCF}$ energy. On the other hand, $E_{\rm int}^{\rm SCF}$ is *repulsive* for MNe($^2\Pi$), although it is attractive over a wide range of R for M$^+$Ne. These SCF-level findings again suggest there exists an additional *repulsive* interaction in MNe($^2\Pi$) that is not present in MHe($^2\Pi$) or in the cations.

Further insight into the repulsive components of the MNe($^2\Pi$) potential curves can be obtained by analyzing $E_{\rm int}^{\rm SCF}$ as a first-order Heitler–London portion, $E_{\rm int}^{\rm HL}$, and a deformation component $E_{\rm int}^{\rm def}$[72]

$$E_{\rm int}^{\rm SCF}=E_{\rm int}^{\rm HL}+E_{\rm int}^{\rm def}. \tag{1}$$

$E_{\rm int}^{\rm HL}$ describes the interaction energy as the energy difference between that of the separated fragments (E_A and E_B) and the energy for a wave function $\psi_{AB}^{\rm HL}$ which is an antisymmetrized product of the SCF wave functions of the *undeformed* A and B fragments: $\psi_{AB}^{\rm HL}=A\psi_A\cdot\psi_B$

$$E_{\rm int}^{\rm HL}=\frac{\langle\psi_{AB}^{\rm HL}|H|\psi_{AB}^{\rm HL}\rangle}{\langle\psi_{AB}^{\rm HL}|\psi_{AB}^{\rm HL}\rangle}-E_A-E_B. \tag{2}$$

$E_{\rm int}^{\rm HL}$ is evaluated in practice in the first iteration of the SCF interaction process before the orbitals of ψ_A and of ψ_B deform due to the presence of the other fragments.

The second term of Eq. (1), $E_{\rm int}^{\rm def}$, has its origin in the mutual deformation of the interacting species,[72] and, for the species considered here, is found to be the *dominant attractive component* of $E_{\rm int}^{\rm SCF}$.

The energy $E_{\rm int}^{\rm HL}$ is commonly decomposed into three pieces:[73] the electrostatic interaction energy $E_{\rm elst}$, an exchange energy $E_{\rm exch}$, and an orbital orthogonality factor E_S

$$E_{\rm int}^{\rm HL}=E_{\rm elst}+E_{\rm exch}+E_S. \tag{3}$$

The component $E_{\rm elst}$ gives the classical (Coulomb) interaction between the charge distributions of A and B. Due to the spherical symmetry of the RG atoms, $E_{\rm elst}$ does not have any long-range multipole components for the systems studied here. The term $E_{\rm exch}$ is given as a *negative* sum of two-electron exchange integrals between pairs of orbitals on A and B. Hence, $E_{\rm exch}$ is negative (attractive). In the final contribution E_S, one- and two-electron integrals are combined with overlap integrals (S) between orbitals of A and of B to produce an overall *repulsive* contribution to $E_{\rm int}^{\rm SCF}$.

The source of additional repulsion in MNe($^2\Pi$) can now be clarified. The $np\pi$ orbital of M has zero overlap with the occupied helium valence $1s$ orbital (by symmetry). As a consequence, the contribution from the $np\pi$ orbital to the interfragment overlap E_S term vanishes, but the attractive contribution in $E_{\rm exch}$ remains. However, for noble gases with s^2p^6 configurations, the (repulsive) $np\pi$ contribution of E_S no longer vanishes, since the $p\pi$ orbitals of the M and RG atoms have nonzero overlap. One therefore expects more repulsive SCF interaction energies for MNe($^2\Pi$) than for M$^+$Ne($^1\Sigma^+$), consistent with our findings.

Also consistent with this interpretation are the differences in π orbital energies observed for LiHe and LiNe (relative to the $2p$ orbital energy of an isolated excited Li atom) at the respective R_e distances. The singly occupied π orbital of LiNe($^2\Pi$) is *destabilized* by ~1000 cm^{-1} relative to isolated Li($2p$), but for LiHe($^2\Pi$) the π orbital is slightly (~100 cm^{-1}) *stabilized.* Due to the intervention of the Pauli exclusion principle, the filled $2p\pi$ orbitals of Ne act to repel the higher energy $2p\pi$ orbital of Li(^2P).

To further test our hypothesis that the absence of occupied $p\pi$ orbitals is what makes the He atom "special" when interacting with M($np\pi$) states, we designed the following numerical experiment. For the noble gases having s^2p^6 configurations, the first M·RG($^2\Delta$) Rydberg-type states should also have vanishing (repulsive) E_S overlap energies. For such states, the M $nd\delta$ orbital contributes nothing to E_S because it is orthogonal to all RG s and p orbitals. Indeed, the SCF potential energy curve we obtain for Li($3d$ ^2D)·Ne($^2\Delta$) has a D_e of 580 cm^{-1} at ~2.2 Å, similar to those for the Li$^+$·Ne cation ground state, where $D_e=700$ cm^{-1} at 2.2 Å. This is in stark contrast, of course, to the Li($2p$ ^2P)·Ne($^2\Pi$) state, which is +360 cm^{-1} *repulsive* at $R=2.2$ Å at the SCF level.

ACKNOWLEDGMENTS

We are grateful for support of this research by the National Science Foundation, Grants Nos. CHE9215335 (W.H.B.) and CHE9116286 (J.S.), and by the Petroleum Research Fund, Award No. 24573 AC6C (W.H.B.). S. B. would like to acknowledge Dr. Alexander Boldyrev for advice and help in using the GAUSSIAN 92 code. We thank Mr. Allen Leung for constructing some of the figures.

[1] C. J. Lee, M. D. Havey, and R. P. Meyer, Phys. Rev. A **43**, 77 (1991).
[2] C. J. Lee and M. D. Havey, Phys. Rev. A **43**, 6066 (1991).
[3] R. Scheps, Ch. Ottinger, G. York, and A. Gallagher, J. Chem. Phys. **63**, 2581 (1975).
[4] M. Jungen and V. Staemmler, J. Phys. B **21**, 463 (1988).
[5] I. R. Gatland, W. F. Morrison, H. W. Ellis, M. G. Thackston, E. W. McDaniel, M. H. Alexander, L. A. Viehland, and E. A. Mason, J. Chem. Phys. **66**, 5121 (1977).
[6] P. Polak-Dingels, M. S. Rajan, and E. A. Gislason, J. Chem. Phys. **77**, 3983 (1982).
[7] A. D. Koutselos, E. A. Mason, and L. A. Viehland, J. Chem. Phys. **93**, 7215 (1990).
[8] L. A. Viehland, Chem. Phys. **78**, 279 (1983).
[9] R. Ahlrich, H. J. Böhm, S. Brode, K. T. Tang, and J. P. Toennies, J. Chem. Phys. **88**, 6290 (1988).
[10] I. Røeggen and H. R. Skullerud, J. Phys. B **25**, 1795 (1992).
[11] I. R. Gatland, J. Chem. Phys. **75**, 4162 (1981).

[12] C. W. Bauschlicher, Jr., H. Partridge, and S. R. Langhoff, Chem. Phys. Lett. **165**, 272 (1990).

[13] R. E. Olson and B. Liu, Chem. Phys. Lett. **62**, 242 (1979).

[14] C. W. Bauschlicher, Jr., H. Partridge, and S. R. Langhoff, J. Chem. Phys. **91**, 4733 (1989).

[15] K. V. Subbaram, J. A. Coxon, and W. E. Jones, Can. J. Phys. **54**, 1535 (1976).

[16] J. A. Coxon, W. E. Jones, and K. V. Subbaram, Can. J. Phys. **55**, 254 (1977); we have estimated D_e for $BeKr^+$ states by $D_e=(\omega_e)^2/4\omega_e x_e$.

[17] W. P. Lapatovich, R. Ahmad-Bitar, P. E. Moskowitz, I. Renhorn, R. A. Gottscho, and D. E. Pritchard, J. Chem. Phys. **73**, 5419 (1980).

[18] R. A. Gottscho, R. Ahmad-Bitar, W. P. Lapatovich, I. Renhorn, and D. E. Pritchard, J. Chem. Phys. **75**, 2546 (1981).

[19] M. D. Havey, S. E. Frolking, and J. J. Wright, Phys. Rev. Lett. **45**, 1783 (1980).

[20] T. Pascale, technical report, Service de Physique des Atoms et des Surfaces (C. E. Saclay), as quoted in R. deVivie-Riedle, J. P. J. Driessen, and S. R. Leone, J. Chem. Phys. **98**, 2038 (1993).

[21] J. Tellinghuisen, A. Ragone, M. S. Kim, D. J. Auerbach, R. E. Smalley, L. Wharton, and D. H. Levy, J. Chem. Phys. **71**, 1283 (1979).

[22] R. Brühl, J. Kapetanakis, and D. Zimmerman, J. Chem. Phys. **94**, 5865 (1991).

[23] P. Baumann, D. Zimmerman, and R. Brühl, J. Mol. Spectrosc. **155**, 277 (1992).

[24] C. W. Bauschlicher, Jr., H. Partridge, and S. R. Langhoff, in *Advances in Metal and Semiconductor Clusters*, edited by M. Duncan (JIA, Greenwich, in press).

[25] C. Nyeland, K. T. Tang, and J. P. Toennies, Chem. Phys. **147**, 229 (1990).

[26] G. Chalasinski and J. Simons, Chem. Phys. Lett. **148**, 289 (1988).

[27] B. Pouilly, B. H. Lengsfield, and D. Yarkony, J. Chem. Phys. **80**, 5089 (1984).

[28] R. R. Bennett, J. G. McCaffrey, and W. H. Breckenridge, J. Chem. Phys. **92**, 2740 (1990).

[29] I. Wallace and W. H. Breckenridge, J. Chem. Phys. **98**, 2768 (1993).

[30] R. R. Bennett, J. G. McCaffrey, I. Wallace, D. J. Funk, A. Kowalski, and W. H. Breckenridge, J. Chem. Phys. **90**, 2140 (1989).

[31] J. G. McCaffrey, D. J. Funk, and W. H. Breckenridge, J. Chem. Phys. **99**, 9472 (1993).

[32] J. S. Pilgrim, C. S. Yeh, and M. A. Duncan, Chem. Phys. Lett. **210**, 322 (1993).

[33] R. R. Bennett and W. H. Breckenridge, J. Chem. Phys. **92**, 1588 (1990).

[34] I. Wallace, J. G. Kaup, and W. H. Breckenridge, J. Phys. Chem. **95**, 8060 (1991).

[35] I. Wallace, R. R. Bennett, and W. H. Breckenridge, Chem. Phys. Lett. **153**, 127 (1988).

[36] I. Wallace, J. Ryter, and W. H. Breckenridge, J. Chem. Phys. **96**, 136 (1992).

[37] A. Kvaran, D. J. Funk, A. Kowalski, and W. H. Breckenridge, J. Chem. Phys. **89**, 6069 (1988).

[38] R. Bobkowski, M. Czajkowski, and L. Krause, Phys. Rev. A **41**, 243 (1990).

[39] M. Czajkowski, R. Bobkowski, and L. Krause, Phys. Rev. A **44**, 5730 (1991).

[40] R. R. Bennett and W. H. Breckenridge, J. Chem. Phys. **96**, 882 (1992).

[41] D. J. Funk, A. Kvaran, and W. H. Breckenridge, J. Chem. Phys. **90**, 2915 (1989).

[42] K. Yamanouchi, S. Isogai, M. Okunishi, and S. Tsuchiya, J. Chem. Phys. **88**, 205 (1988).

[43] M. Okunishi, H. Nakazawa, K. Yamanouchi, and S. Tsuchiya, J. Chem. Phys. **93**, 7526 (1990).

[44] M.-C. Duval, O. Benoist d'Azy, W. H. Breckenridge, C. Jouvet, and B. Soep, J. Chem. Phys. **85**, 6324 (1986).

[45] T. Tsuchizawa, K. Yamanouchi, and S. Tsuchiya, J. Chem. Phys. **89**, 4646 (1988).

[46] S. H. Linn, J. M. Brom, Jr., W.-B. Tzeng, and C. Y. Ng, J. Chem. Phys. **82**, 648 (1985).

[47] N. Bridge and J. James, J. Mol. Spectrosc. **42**, 370 (1972).

[48] C. Dedonder-Lardeux, C. Jouvet, M. Richard-Viard, and D. Solgadi (to be published).

[49] C. L. Liao and C. Y. Ng, J. Chem. Phys. **84**, 1142 (1986).

[50] W. H. Breckenridge, C. Jouvet, and B. Soep, in *Advances in Metal and Semiconductor Clusters*, Vol. III, edited by M. Duncan (JIA, Greenwich, to be published).

[51] J. P. Desclaux, At. Data Nucl. Tables **12**, 311 (1973).

[52] J. O. Hirschfelder, C. F. Curtiss, and R. B. Bird, *Molecular Theory of Gases and Liquids* (Wiley, New York, 1964).

[53] J. S. Binkley, M. J. Frisch, D. J. DeFrees, K. Keghavachri, R. A. Whiteside, H. B. Schlegel, E. M. Fluder, and J. A. Pople, GAUSSIAN 92 (Carnegie-Mellon University, Pittsburgh, 1992).

[54] M. Dupuis, D. Spangler, and J. J. Wendolowski, National Resource for Computations in Chemistry Software Catalog, University of California, Berkeley, CA (1980), Program QG01; M. W. Schmidt, K. K. Baldridge, J. A. Boatz, J. H. Jensen, S. Koseki, M. S. Gordon, K. A. Nguyen, T. L. Windus, and S. T. Elbert, QCPE Bull. **10**, 52 (1990).

[55] R. Krishnan, J. S. Binkley, R. Seeger, and J. A. Pople, J. Chem. Phys. **72**, 650 (1980).

[56] A. D. McLean and G. S. Chandler, J. Chem. Phys. **72**, 5639 (1982).

[57] T. H. Dunning and P. J. Hay, *Methods of Electronic Structure Theory*, edited by H. F. Shaefer (Plenum, New York, 1977), Ch. 1, pp. 1–28.

[58] W. Wadt and P. Hay, J. Chem. Phys. **82**, 184 (1985).

[59] J. Andzelm, M. Klobukowski, E. Radzio-Andzelm, Y. Sakai, and H. Tateraki, *Gaussian Basis Sets for Molecular Calculations*, edited by S. Huzinaga, Physical Science Data 16 (Elsevier, Amsterdam, 1984).

[60] T. H. Dunning, J. Chem. Phys. **55**, 716 (1971).

[61] *The General Atomic and Molecular Electronic Structure Systems: HONDO 7.0*, M. Dupuis, J. D. Watts, H. O. Villar, and G. J. B. Hurst, Comput. Phys. Comm. **52**, 415 (1989).

[62] M. J. Frisch, J. A. Pople, and J. S. Binkley, J. Chem. Phys. **80**, 3265 (1984).

[63] W. J. Stevens, H. Basch, and M. Krauss, J. Chem. Phys. **81**, 6026 (1984).

[64] M. Gutowski and J. Simons, J. Chem. Phys. **93**, 3874 (1990).

[65] S. F. Boys and F. Bernardi, Mol. Phys. **19**, 553 (1970).

[66] R. J. Vos, J. H. van Lenthe, and F. B. van Duijneveldt, J. Chem. Phys. **93**, 643 (1990).

[67] J. Sadlej and W. D. Edwards, Int. J. Quantum Chem. Quantum Chem. Sympos. **27**, 731 (1993).

[68] A report of very early SCF calculations (Ref. 69) indicated the facile penetration by the He atom of the $Li(2p\pi)$ orbital in the $LiHe(^2\Pi)$ state. It was also found in that work (Ref. 69) and later calculations (Ref. 4) that the $Li\cdot He(^2\Pi)$ and $Li^+\cdot He$ potential curves were similar near their R_e values at the SCF level.

[69] M. Krauss, P. Maldonado, and A. C. Wahl, J. Chem. Phys. **54**, 4944 (1971).

[70] G. D. Mahan, J. Chem. Phys. **50**, 2755 (1969).

[71] K. T. Tang and J. P. Toennies, J. Chem. Phys. **80**, 3726 (1984).

[72] M. Gutowski and L. Piela, Mol. Phys. **64**, 337 (1988).

[73] P.-O. Löwdin, Adv. Phys. **5**, 1 (1956).